*Journal of Structural Chemistry. Vol. 58, No. 3, pp. 539-543, 2017.*


# CRYSTAL STRUCTURE AND PROPERTIES OF POLYMERIC HEXAAQUA-*hexakis*-(2-THIOBARBITURATO)-DISAMARIUM(III)

**N. N. Golovnev[1], M. S. Molokeev[2,3], I. V. Sterkhova[4], S. N. Vereshchagin[5], and I. I. Golovneva[6]**

UDC 541.49:548.73

The structure (CIF file CCDC No. 1401886) of the hexaaqua-*hexakis*(2-thiobarbiturato)-disamarium $[Sm_2(H_2O)_6(HTBA)_6]_n$ polymeric complex (**I**), where $H_2TBA$ is 2-thiobarbituric acid, is determined; its thermal decomposition and IR spectrum are studied. The crystals of **I** are monoclinic: $a = 14.072(1)$ Å, $b = 10.0842(6)$ Å, $c = 15.323(1)$ Å, $\beta = 110.408(2)°$, $V = 2037.9(2)$ Å$^3$, space group $P2/n$, $Z = 2$. All three independent thiobarbiturate anions $HTBA^-$ coordinate to $Sm^{3+}$ through oxygen atoms. To one of independent $Sm^{3+}$ ions six (two terminal and four bridging) $HTBA^-$ ions and two water molecules are coordinated; the second is bonded with four bridging $HTBA^-$ and four water molecules, forming square antiprisms. The bridging $HTBA^-$ anions arrange antiprisms in layers. The structure is stabilized by hydrogen bonds and a π–π interaction between the $HTBA^-$ ions. The topology of the polymer network of **I** is analyzed.

**DOI:** 10.1134/S0022476617030155

**Keywords:** structure, synthesis, complex, 2-thiobarbituric acid, samarium(III), thermal decomposition, IR spectrum.

Samarium compounds are considered as promising dopants in fuel cells [1], photoluminescent materials [2], and catalysts [3]. They are becoming increasingly important in the organic synthesis of polyfunctional substances [4].

This work reports the results of the synthesis, thermal and IR spectroscopic studies of a new Sm(III) complex with 2-thiobarbituric acid ($H_2TBA$). It is a promising precursor for producing $Sm_2S_3$ sulfide and $Sm_2O_2SO_4$ dioxosulfate. The first of these compounds can be used in supercondensers [1], and the second, as an oxygen source in different chemical processes and materials science [5]. Oxysulfates of rare-earth metals are active and stable catalysts of a hydrogen generation reaction by water-gas shift conversion [6] and underlie the synthesis of anaerobic oxidative systems [7].

## EXPERIMENTAL

0.128 g (0.232 mmol) of chemically pure $Sm_2CO_3 \cdot 4H_2O$ were dissolved in 10 ml of water, then 0.200 g (1.39 mmol) of chemically pure solid $H_2TBA$ were added portionwise at 60°C. In 8 h, the yellow-brown fine crystalline precipitate formed

[1]Siberian Federal University, Krasnoyarsk, Russia; ngolovnev@sfu-kras.ru. [2]Kirensky Institute of Physics, Siberian Branch, Russian Academy of Sciences, Krasnoyarsk, Russia. [3]Far Eastern State Transport University, Khabarovsk, Russia. [4]Favorsky Institute of Chemistry, Siberian Branch, Russian Academy of Sciences, Irkutsk, Russia. [5]Institute of Chemistry and Chemical Technology, Siberian Branch, Russian Academy of Sciences, Krasnoyarsk, Russia. [6]Krasnoyarsk State Agrarian University, Russia. Translated from *Zhurnal Strukturnoi Khimii*, Vol. 58, No. 3, pp. 567-571, March-April, 2017. Original article submitted January 12, 2016; revised August 11, 2016.

was filtered, washed with ethanol, and dried in the air. On slow evaporation of the filtrate, single crystals of a new phase $[Sm_2(H_2O)_6(HTBA)_6]_n$ (**I**) were obtained.

**Single crystal XRD study.** A 0.35×0.28×0.14 mm yellow crystal of **I** was examined at 296 K. The reflection intensities were measured on a D8 Venture single crystal diffractometer (the equipment of the Baikal Analytical Center for Collective Use, Siberian Branch, Russian Academy of Sciences), Mo$K_\alpha$ radiation, λ = 0.7106 Å. Experimental absorption corrections were applied using the SADABS software [8] by multiscanning. The model of the structure was found by direct methods and refined using the SHELXTL software [9]. From the difference electron density maps, the positions of hydrogen atoms were determined, which were then idealized and refined with reference to the main atoms. The main crystallographic characteristics and the parameters of the experiment are as follows: $M_r$ = 1267.66, $a$ = 14.072(1) Å, $b$ = 10.0842(6) Å, $c$ = =15.323(1) Å, β = 110.408(2)°, $V$ = 2037.9(2) Å$^3$, space group $P2/n$, $Z$ = 2, $D_x$ = 2.066 g/cm$^3$, μ = 3.249 mm$^{-1}$, $2\theta_{max}$ = 60.23°; in total, 83043 reflections, 6001 independent reflections, $R_B$ = 3.28%, $wR(F^2)$ = 5.33%, $\Delta\rho_{max}/\Delta\rho_{min}$ = 1.807/–1.127 e/Å$^3$.

The structure of **I** has been deposited with the Cambridge Structural Database (No. 1401886; deposit@ccdc.cam.ac.uk or http://www.ccdc.cam.ac.uk/data_request/cif).

The IR spectrum of **I** in KBr in a range 4000-400 cm$^{-1}$ was recorded on a FTIR Nicolet 6700 spectrometer. The synchronous thermal analysis was performed on a Netzsch STA Jupiter 449C device combined with an Aeolos QMS 403C mass spectrometric analyzer in a flow of the 20% $O_2$–Ar mixture in a platinum crucible with a perforated cover; a portion weight was 4.15 mg. The temperature program included a segment of temperature stabilization at 40°C for 30 min, which was followed by heating to 900°C with a rate of 10°C·min$^{-1}$. The qualitative composition of effluent gases was determined by a change in the intensity of ions with $m/z$ = 18 ($H_2O$), 28 ($N_2$, CO), 30 (NO), 32 ($O_2$), 44 ($CO_2$), 60 (COS), and 64 ($SO_2$, $SO_3$).

## RESULTS AND DISCUSSION

The asymmetric part of the unit cell of **I** contains two $Sm^{3+}$ ions in special positions 2*e* and 2*f*, three $HTBA^-$ ions, and three water molecules in general positions. Two independent $Sm^{3+}$ positions have the same symmetry – the twofold axis, but the coordination environment of the ions is different (Figs. 1 and 2).

One of the $Sm^{3+}$ ions is bonded with six (two terminal and four bridging) $HTBA^-$ ions and two water molecules, the second ion is bonded with four bridging $HTBA^-$ and four water molecules. The $HTBA^-$ ions coordinate to the $Sm^{3+}$ ions only through O atoms. The Sm–O bond lengths (2.344(2)-2.515(2) Å) are typical of Sm(III) complexes [10]. The structure contains three independent $HTBA^-$ ions: one terminal (**C**) and two bridging (**A** and **B**). Their corresponding geometric parameters are almost identical; for example, the bond lengths of C–O (1.257(3)-1.276(3) Å), C(4)–C(5) and C(5)–C(6) (1.393(3)-1.399(3) Å), and C–C (1.682(3)-1.689(3) Å). The similarity of all C–O distances indicates electron density delocalization in the O=C–CH–C=O atomic groups (Fig. 1). Both $Sm1O_8$ and $Sm2O_8$ polyhedra are square antiprisms bridged by $HTBA^-$ with the formation of an infinite layer in the plane perpendicular to the $a+c$ direction. As in the

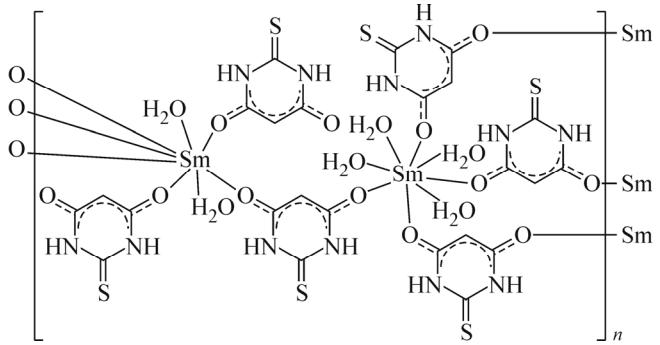


**Fig. 1.** Structure of the $[Sm_2(H_2O)_6(HTBA–O,O')_4 \cdot (HTBA–O)_2]_n$ complex.

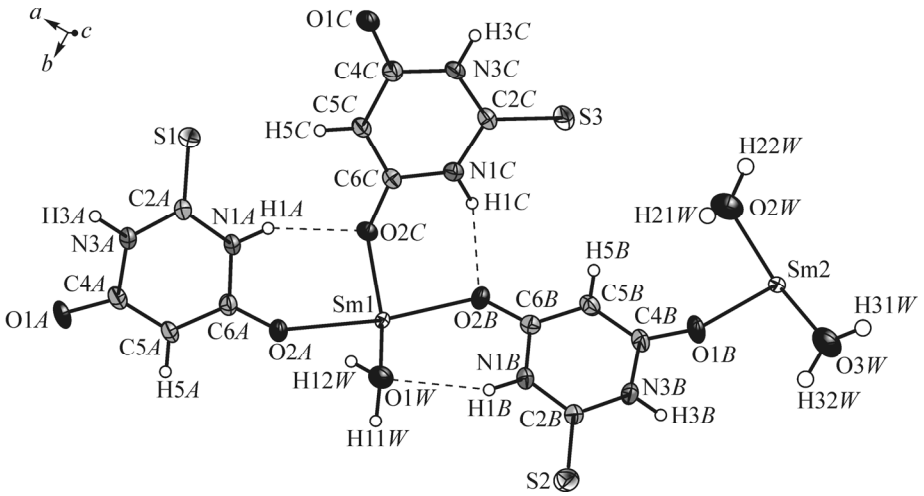


**Fig. 2.** Asymmetric part of the unit cell of **I**. Hydrogen bonds are shown by dashed lines.

isostructural $[Eu_2(H_2O)_6 \cdot (HTBA)_6]_n$ complex [11], a 24-membered ring containing both Sm(1) and Sm(2) atoms forms in this layer. The N–H…O, N–H…S, O–H…O, and O–H…S hydrogen bonds (Table 1) form a three-dimensional framework. The calculated intercentroid distances [13] of 3.940(1) Å and 3.742(1) Å indicate a head-to-tail π–π interaction of the $HTBA^-$ ions [12].

The topological analysis of the polymer network formed by the bridging $HTBA^-$ ions was performed [14]. To this end, all $HTBA^-$ ions were replaced by spheres located in the centers of their rings, and the terminal water molecules and the $HTBA^-$ ions were not taken into account. As a result, each of the Sm1 and Sm2 ions appeared to be coordinated by four $HTBA^-$ ligands, and each $HTBA^-$ ion appeared to be bonded with two $Sm^{3+}$ ions. Hence, Sm1 and Sm2 act as four-coordinated sites, and the $HTBA^-$ ions act as two-coordinated sites (Fig. 3*a*). The Sm1 and Sm2 ions are crystallographically independent, but topologically equivalent, as all $HTBA^-$ sites. Therefore, the two-dimensional polymer network presented is a (4,2)-connected binodal net with the Schlafli symbol of $(8^4.12^2)(8^2)$. The $HTBA^-$ ions are only two-coordinated sites and if we remove them (Fig. 3*b*), we get a common square lattice consisting only of $Sm^{3+}$ ions with the Schlafli symbol of $(4^4.6^2)$.

The IR spectrum of **I** (ν, $cm^{-1}$) is as follows: 3500-2800m (broad band), 1698m, 1639vs, 1519s, 1444w, 1376s, 1308s, 1166s, 1157s, 1012vw, 936vw, 848vw, 801w, 636vw, 536s, 462m (vw is very weak, w is weak, m is medium, s is

**TABLE 1.** Geometric Parameters of Hydrogen Bonds in the Structure of **I**

| D–H···A contact | Distance, Å | | | DHA angle, deg | Transformation for A atom |
|---|---|---|---|---|---|
| | D–H | H···A | D···A | | |
| N(1*A*)–H(1*A*)···O(2*C*) | 0.86 | 2.13 | 2.921(3) | 153 | *x*, *y*, *z* |
| N(1*B*)–H(1*B*)···O(1*w*) | 0.86 | 2.31 | 3.087(3) | 151 | *x*, *y*, *z* |
| N(1*C*)–H(1*C*)···O(2*B*) | 0.86 | 2.03 | 2.785(3) | 146 | *x*, *y*, *z* |
| N(3*A*)–H(3*A*)···S(2)$^{i}$ | 0.86 | 2.49 | 3.342(3) | 173 | *x*+1, *y*, *z* |
| N(3*B*)–H(3*B*)···S(1)$^{ii}$ | 0.86 | 2.39 | 3.241(2) | 168 | *x*–1, *y*, *z* |
| N(3*C*)–H(3*C*)···O(1*C*)$^{iii}$ | 0.86 | 2.06 | 2.894(3) | 162 | –*x*+2, –*y*–1, –*z*+1 |
| O(1*W*)–H(11*W*)···S(3)$^{iv}$ | 0.95(2) | 2.35(2) | 3.267(2) | 163(2) | *x*, *y*+1, *z* |
| O(1*W*)–H(12*W*)···O(1*C*)$^{v}$ | 0.94(2) | 1.81(2) | 2.717(3) | 163(3) | –*x*+2, –*y*, –*z*+1 |
| O(2*W*)–H(21*W*)···S(2)$^{vi}$ | 0.95(2) | 2.30(2) | 3.236(2) | 167(2) | –*x*+1,–*y*, –*z*+1 |
| O(2*W*)–H(22*W*)···S(2)$^{vii}$ | 0.95(2) | 2.35(2) | 3.280(2) | 166(2) | *x*, *y*–1, *z* |
| O(3*W*)–H(31*W*)···O(1*C*)$^{ii}$ | 0.95(3) | 2.04(3) | 2.936(3) | 157(3) | *x*–1, *y*, *z* |
| O(3*W*)–H(32*W*)···S(1)$^{ii}$ | 0.96(1) | 2.29(2) | 3.221(3) | 166(2) | *x*–1, *y*, *z* |

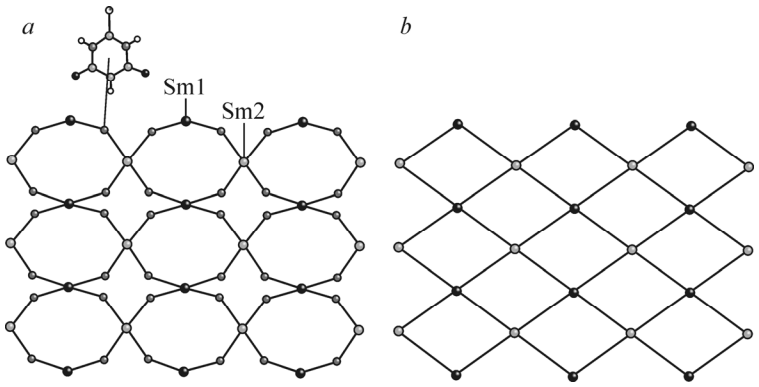


**Fig. 3.** Topological representation of the polymer network in $Sm(Htba)_3(H_2O)_3$ as: the (4,2)-connected binodal net $(8^4.12^2)(8^2)$, where one site is the $Htba^-$ ion and the others are the $Sm^{3+}$ ions (*a*); the 4-connected uninodal net $(4^4.6^2)$ consisting only of $Sm^{3+}$ (*b*).

strong, and vs is very strong). For six $H_2$TBA polymorphs [15], the highest-frequency band ν(CO) is in a range 1705-1750 $cm^{-1}$, and the ν(CS) frequency varies from 1145 $cm^{-1}$ to 1165 $cm^{-1}$ [16]. For **I**, the ν(CO) value is noticeably lower (1698 $cm^1$) than that for $H_2$TBA, which agrees with the $HTBA^-$ coordination through the O atoms. The retention of the ν(CS) band at 1157 $cm^{-1}$ indicates the absence of ligand coordination through the S atom. Therefore, the IR spectroscopy results agree with the powder XRD data.

According to the thermal analysis data, on heating, the transformation of complex **I** occurs in several stages (Fig. 4, Table 2).

In a range 100-280°C, dehydration with a 8.34% weight loss (Δ*m*) occurs, which is close to the calculated value (8.52%) corresponding to the removal of three $H_2O$ molecules. A lower experimental Δ*m* value is likely to be due to a partial removal of water when the sample is kept at 40°C for 30 min. In an oxidizing atmosphere, the organic part of complex **I** is stable up to 280-290°C. At the second stage (~300°C), a significant weight decrease is observed, which is accompanied by heat release and the formation of gaseous oxidation products $H_2O$, $CO_2$, COS, $SO_2$ with the appearance of the corresponding ions with *m*/*z* = 18, 44, 60, and 64 in the mass spectrum (Fig. 5, Table 2). A partial carbonization of the unreacted portion of the compound occurs; the weight loss in this region is about 37%. At the third stage, which is also exothermic, the carbonized residue is additionally oxidized at 480-620°C. This stage is characterized by a significant intensity of ions with *m*/*z* = 44 and 30, a reduced intensity of ions with *m*/*z* = 18, and practically the absence of ions with *m*/*z* = 64; the total weight loss is ~53%.

The last stage of the transformation is an exothermic process of oxidation of the strongly carbonized residue, which, in addition to C, contained N and S (Table 2). According to the TG analysis data (Fig. 4), the total weight loss Δ*m* on heating of **I** to 900°C is 63.24%, which is lower than the theoretic value for process (1)

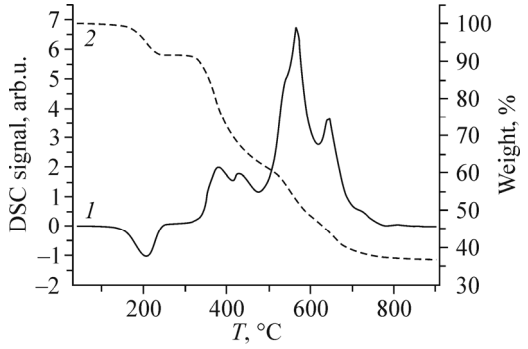


**Fig. 4.** DSC (*1*) and TG (*2*) curves on the oxidative degradation of **I**.

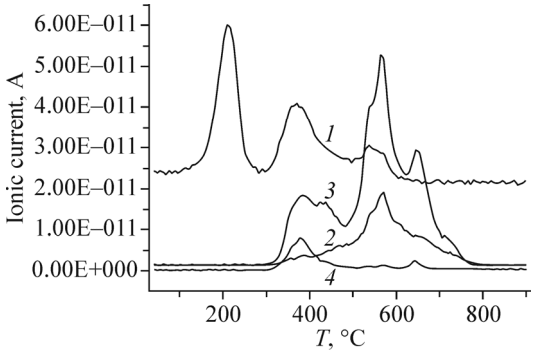


**Fig. 5.** Intensities of the ionic masses with *m*/*z* 18 (*1*), 30 (*2*), 44 (*3*), and 64 (*4*) on the oxidative decomposition of **I**.

**TABLE 2.** Temperature Ranges of Transformation, Weight Loss, and the Intensities of the Main Ions on the Oxidative Decomposition of Complex **I**

| Stage | $T$, °C | $\Delta m$, % | $m/z$ | | | | |
|---|---|---|---|---|---|---|---|
| | | | 18 ($H_2O$) | 30 (NO) | 44 ($CO_2$) | 60 (COS) | 64 ($SO_2$) |
| 1 | 100-280 | 8.32 | +++ | ( – ) | ( – ) | ( – ) | ( – ) |
| 2 | 290-480 | 37 | ++ | ( – ) | ++ | + | ++ |
| 3 | 480-620 | 53 | + | ++ | +++ | ( – ) | ( – ) |
| 4 | 620-900 | 63.24 | ( – ) | + | ++ | ( – ) | + |

+++ is the main product; the number of (+) symbols corresponds to the relative ionic current intensity; ( – ) means almost no signal.

$$Sm_2(H_2O)_6(HTBA)_3 \rightarrow Sm_2O_2SO_4 \cdot \Delta m_{theor.} = 66.18\%. \quad (1)$$

This discrepancy is most likely to be caused by an incomplete decomposition of the intermediate compound $Sm_2(HTBA)_3$ to $Sm_2O_2SO_4$ under limited time of the TG analysis [5, 6]. According to the powder XRD data, after heating complex **I** at 800°C for 2 h, the residue contained the pure $Sm_2O_2SO_4$ phase, similarly to the previous result of the $Nd(H_2O)_2(HTBA)_2(C_2H_3O_2)\cdot 2H_2O$ thermal decomposition when pure $Nd_2O_2SO_4$ was obtained [17].

The work was performed at the Siberian Federal University within the state task of the Ministry of Education and Science of the Russian Federation for 2014-2016 (Project No. 3049).

## REFERENCES

1. V. S. Kumbhar, A. C. Lokhande, N. S. Gaikwad, and C. D. Lokhande, *Mater. Sci. Semicond. Process.*, **33**, 136-139 (2015).
2. D. J. Park, T. Sekino, S. Tsukuda, et al., *J. Solid State Chem.*, **184**, 2695-2700 (2011).
3. F. C. G. Mattos, J. A. S. Souza, and A. B. A. Cotrim, *Appl. Catal.*, *A*, **423/424**, 1-6 (2012).
4. M. Szostak, N. J. Fazakerley, D. Parmar, and D. J. Procter, *Chem. Rev.*, **114**, No. 11, 5959-6039 (2014).
5. J. A. Poston Jr., R. V. Siriwardane, E. P Fisher, et al., *Appl. Surf. Sci.*, **214**, 83-102 (2003).
6. I. Valsamakis and M. Flytzani-Stephanopoulos, *Appl. Catal.*, **B106**, 255-263 (2011).
7. K. Ikeue, M. Eto, D.-J. Zhang, et al., *J. Catal.*, **248**, 46-52 (2007).
8. G. M. Sheldrick, *SADABS. Version 2.01*, Bruker AXS Inc., Madison, WI, USA (2004).
9. G. M. Sheldrick, *SHELXTL. Version 6.10*, Bruker AXS Inc., Madison, WI, USA (2004).
10. *Cambridge Structural Database. Version 5.36*, Univ. of Cambridge, Cambridge, UK (2014).
11. N. N. Golovnev and M. S. Molokeev, *Russ. J. Coord. Chem.*, **40**, No. 9, 648-652 (2014).
12. J. L. Atwood and J. W. Steed, *Supramolecular Chemistry*, VCH, Weinheim, Germany (2000).
13. *PLATON. A Multipurpose Crystallographic Tool*, Utrecht Univ., Utrecht, Netherlands (2008).
14. S. R. Batten, S. M. Neville, and D. R. Turner, *Coordination Polymers: Design, Analysis and Application*, Royal Society of Chemistry, Cambridge (2009).
15. M. R. Chierotti, L. Ferrero, N. Garino, et. al., *Chem. Eur. J.*, **16**, 4347-4358 (2010).
16. N. N. Golovnev and M. S. Molokeev, *2-Thiobarbituric Acid and its Complexes with Metals: Synthesis, Structure, and Properties* [in Russian], Sib. Feder. Univ, Krasnoyarsk (2014).
17. N. N. Golovnev, M. S. Molokeev, S. N. Vereshchagin, and V. V. Atuchin, *J. Coord. Chem.*, **68**, No. 11, 1865-1877 (2015).